BMC Immunology

RESEARCH

Open Access

HTLV-1-infected cells drive the differentiation of monocytes into macrophages in vitro

Sabrina de Souza[1], Guilherme Affonso Melo[2], Carolina Calôba[2], Maria Clara Salgado Campos[1], Juliana Vieira Pimenta[1], Fabianno Ferreira Dutra[3], Renata Meirelles Pereira[2] and Juliana Echevarria-Lima[1,4*]

Abstract

Background The human T-cell lymphotropic virus type 1 (HTLV-1) is a retrovirus that causes HTLV-1-associated myelopathy/tropical spastic paraparesis (HAM/TSP). HAM/TSP is a chronic inflammatory neurodegenerative disease characterized by leukocyte infiltration in the spinal cord. T-lymphocytes are the most important targets of HTLV-1 infection, but monocytes are also infected. Monocytes from HTLV-1-infected individuals exhibit important functional differences compared to cells from uninfected donors. Here, we investigated the effects of cell-cell physical contact and/or secreted factors of HTLV-1-infected cells in monocyte activation and differentiation.

Methods The THP-1 human monocytic cell line was co-cultured with a human cell line transformed by HTLV-1 (MT-2) for 6 days. To determine the effects of co-culturing HTLV-1-infected cells in THP-1 monocytes cells were characterized by flow cytometry, immunofluorescence microscopy, and real-time PCR. Computational analysis of published transcriptomic datasets was realized to compare molecular profiles of macrophages and mononuclear cells from HTLV-1 carriers.

Results Co-culture of monocytes with HTLV-1-infected cells induced macrophage differentiation and upregulation of typical macrophages-associated molecules (HLA-DR, CD80, and CD86), increased cytokine (TNFα, IL-6, and IL-1β) levels and their coding genes expression. Consistently, published transcriptomic datasets showed changes in important genes associated with inflammation during HAM/TSP in patients. The presence of HTLV-1-infected cells in the culture also induced significant upregulation of Interferon Stimulated Genes (ISG), indicating viral infection. Monocyte activation and differentiation into pro-inflammatory macrophages occurred in a cell-to-cell contact-independent manner, suggesting the role of factors secreted by infected cells.

Conclusions Together, our results indicated that HTLV-1-infected cells induced monocyte differentiation into macrophages inflammatory, predominantly.

Keywords HTLV-1, Monocyte, Macrophage, Cell differentiation, Inflammatory phenotype

*Correspondence:
Juliana Echevarria-Lima
juechevarria@micro.ufrj.br
Full list of author information is available at the end of the article

Background

The human T-cell lymphotropic virus type 1 (HTLV-1) is a retrovirus associated with myelopathy/tropical spastic paraparesis (HAM/TSP) and adult T leukemia/lymphoma (ATLL) [1, 2]. HTLV-1 is endemic and widely distributed among different ethnicities and regions, prevailing in Africa, Japan, and Central and South America. Worldwide, it is estimated that around 15 to 20 million individuals are living with HTLV-1 [3]. HAM/TSP is a chronic inflammatory disease characterized by leukocyte infiltration into the spinal cord, causing degeneration and loss of motor capacity [4, 5]. HAM/TSP patients can present spastic paraparesis followed by sphincter alterations, peripheral neuropathy, low back pain, erectile dysfunction, cognitive and dysautonomic alterations, and loss of myelin sheath and axons [6–8].

HTLV-1 primarily infects T $CD4^+$ lymphocytes [9, 10], but can also infect other cells, such as T $CD8^+$ lymphocytes [11], natural killer cells [12], dendritic cells [13], monocytes, and macrophages [14–17], including colostrum macrophages [18].

According to the bystander model, described by Bangham (2015), infected cells and activated HTLV-1-specific lymphocytes cross the blood-brain barrier and induce an inflammatory response by IFN-γ, TNF-α, and IL-6 production [19]. IFN-γ stimulates astrocytes to secrete CXCL10, attracting $CX3CR1^+$ lymphocytes and phagocytes to the Central Nervous System (CNS) [20, 21]. Consequently, these leukocytes induce glial stress, demyelination, and destruction of axons [19].

Monocytes play an important role in neurodegenerative diseases but are under-investigated during HTLV-1 HAM/TSP. Generally, these cells infiltrate into the CNS after the blood-brain barrier breaks [22] and differentiate into dendritic cells and M1 (classic) macrophages promoting inflammation [23]. The impairment of monocyte-derived dendritic cells during HTLV-1 infection has been described. Monocytes obtained from infected individuals and stimulated in vitro with GM-CSF and IL-4 have a reduced capacity to differentiate into dendritic cells compared to non-infected individuals [16]. Moreover, a lower frequency of these cells has been observed in ATLL and HAM/TSP patients [24, 25].

Ziegler-Heitbrock (1989) divided monocytes into three groups according to the expression of CD14 and CD16 (FcRγIII): classical ($CD14^{high}CD16^{neg}$), intermediate ($CD14^+CD16^+$), and non-classical ($CD14^{low/neg}CD16^{high}$) [26]. In patients with acquired immunodeficiency syndrome (AIDS), intermediate monocytes ($CD14^+CD16^+$) expand during HIV-1-associated dementia [27, 28]. De Castro-Amarante et al. (2015) showed that classical monocytes obtained from individuals with HTLV-1 express higher levels of chemokine receptors CCR5, CXCR3, and CX3CR1 [29]. This evidence suggests that intermediate monocytes could carry this virus to the CNS [30, 31]. Enose-Akahata et al. (2012) observed the presence of phagocytes expressing high levels of HLA-DR and CX3CR1 in spinal cord injuries of individuals with HAM/TSP [21]. Using proteomic analysis, our group revealed important changes in the expression of cytoskeletal proteins in monocytes of HTLV-1 carriers, demonstrating an increase in proteins associated with adhesion and migration phenomena, such as gelsolin [17].

This study investigated the phenotypic and functional profile of monocyte cell line (THP-1) co-cultured with HTLV-1 permanently infected cells. We showed that HTLV-1-infected cells induce a macrophage differentiation in vitro, characterized by the expression of molecules associated with M1-like phenotype, predominantly, but also with M2-like molecules up-regulated. The comparison of published transcriptomic datasets highlighted inflammatory-associated genes on monocytes and macrophages' transcriptional signatures from HTLV-1 infected individuals, corroborating our in vitro model. Our study can contribute to understanding the immunopathogenesis of HTLV-1-associated diseases.

Methods

Cell culture and THP-1 differentiation

HTLV-1 transformed cell line MT-2 [32] was a gift from Instituto Nacional de Infectologia Evandro Chagas, Fundação Oswaldo Cruz, RJ, Brazil, and monocytic cell line (THP-1) was gently donated by Dr. Ulisses Lopes from Instituto de Biofísica Carlos Chagas Filho of UFRJ. All cells were cultured in Roswell Park Memorial Institute (RPMI)−1640 medium (Lonza) supplemented with 10% fetal bovine serum (FBS) (Gibco/Thermo Fisher), penicillin (100 UI/ml), and streptomycin (100 mg/ml; LGC Biotechnology, Brazil) (complete medium). Cells were cultivated at 37 °C in a humidified atmosphere with CO_2 5% and were passed twice a week.

To induce macrophage differentiation, THP-1 cells were incubated in the presence of 50 ng/ml of Phorbol 12-myristate-13-acetate (PMA; Sigma-Aldrich/Merck) for 72 h in a 37 °C humidified atmosphere with CO_2 5%. Then, cells were washed with PBS (Sigma-Aldrich/Merck) and incubated with a fresh complete medium under the same conditions [33]. Concurrently, THP-1 monocytes were co-cultured with MT-2 cells, previously irradiated (20 Gy) in a 1:2 ratio in a complete medium or the presence of a conditioned medium from MT-2 or THP-1 cells for 6 days at 37 °C in a humidified atmosphere with CO_2 5%.

To evaluate the cell-contact dependence, THP-1 cells were co-cultured with MT-2 cells (1:2 ratio), as described anteriorly [34, 35], in the presence or absence of an insert

(0,47 cm^2 0.4 μm pore; Thermo Fisher Scientific) in a complete medium. After 6 days at 37 °C in a humidified atmosphere with CO_2 5%, the supernatants were collected, and the wells were harvested for phenotypic and/or molecular assay.

Cell viability assay

Cell viability was assessed using MTT (3-[4,5-dimethylthiazol-2-yl])−2,5-diphenyl tetrazolium bromide (5 mg/mL; Sigma-Aldrich/Merk) and Lactate dehydrogenase (LDH; Invitrogen®) assay, according to the manufacturer's instructions. Both assays were performed by colorimetry in a SpectraMax® Paradigm® microplate reader (Molecular Devices) at 490 nm wavelength.

Cell morphology

Cell images were captured through phase-contrast microscopy with magnification objectives 20 and 40. The image analysis system consisted of a light microscope (Olympus CKX41) and a charge-coupled device color camera connected to a computer. All images were stored as TIFF files, using Olympus cell Sens. Image analysis was performed using the ImageJ software.

Phenotype characterization

To determine the effects of co-culturing HTLV-1-infected cells in THP-1 monocytes we characterize the cell phenotype by flow cytometry and immunofluorescence microscopy. After the co-culture period, supernatant was collected and attached cells were washed twice with PBS. For flow cytometry analyses, adherent cells were then detached and incubated for 30 min, on ice, in PBS with 1 mM of EDTA (Sigma-Aldrich/Merck). Cells were stained with anti-human CD14 FITC (clone 61D3, Bioscience), CD80 PE (clone 307.4), CD86 PE (clone 307.4), HLA-DR APC (clone G46-6), CD127 PE-Cy7 (clone HIL-7R-M21) and CD32 PE (clone 3D3), all obtained from BD Pharmigen, for 30 min on ice. For intracellular staining, cells were permeabilized using eBioscence (ThermoFisher) Permeabilization buffer according to the manufacturer's instructions. Then, cells were stained with polyclonal rabbit IgG anti-WARS (Invitrogen/ThermoFisher, PA5-29102) for 30 min at room temperature. After that, cells were washed with permeabilization buffer and labeled with a secondary anti-rabbit IgG polyclonal antibody conjugated to fluorochrome Alexa Fluor 488 (ThermoFisher Scientific, A-11034). Then, cells were washed and acquired on FACSCallibur™ or FACSCanto™ (Beckton & Dickinson). Twenty thousand events were acquired gating forward scatter vs. sideward scatter properties to exclude debris and doublets. Frequency and mean fluorescence intensity (MFI) were assessed by FlowJo 10.0 Software.

For immunofluorescence analyses, cells were also plated in glass coverslips and, after the differentiation process, were fixed with paraformaldehyde 4% (Sigma-Aldrick/Merck) overnight at 4 °C. After washing, cells were permeabilized using Permeabilization buffer (eBioscience®) according to the manufacturer's instructions and blocked with FBS 2% for 2 h at room temperature. Then, samples were stained with CD68 FITC (clone eBioY1/82A; eBioscience®) overnight at 4 °C in a humid chamber. After 3 washes with PBS, the nucleic acids were stained with 1 μg/mL of 4′,6-Diamidino-2-phenylindole dihydrochloride (DAPI; Sigma-Aldrich/Merck) for 1 min at room temperature. Slides were mounted with 30 μL Fluoromount (Sigma-Aldrich/Merck) antifade reagent and analyzed on Leica® or Nikon Eclipse Ti2 fluorescence microscope. Image analyses were performed using the mean fluorescence intensity in the Image J Software.

Cytokine production

Tumor necrosis factor alpha (TNF-α; R&D System), Interleukin-6 (IL-6; R&D System), and CXCL10 (Invitrogen/Thermo) production were analyzed in THP-1 supernatant from control groups and MT-2/THP1 co-cultured cells using sandwich immunosorbent assay (ELISA) kit according to the manufacturer's instructions.

Western blot

THP-1 cells were co-culture in the absence or presence of irradiated THP-1 or MT-2 cells for 6 days at 37 °C and 5% CO_2. After this period, nonadherent cells were removed by washing with phosphate-buffered saline (PBS). The remaining adherent cells were lysed in RIPA buffer (150 mM NaCl, 20 mM Tris-Cl pH 8.0, 0.1% sodium dodecyl sulfate (SDS), 0.5% sodium deoxycholate and 1% NP-40 supplemented with 1× complete protease inhibitors (Roche) and 5 mM iodoacetamide) and kept at −20°C until further use. Cell lysates were spun down at 14,000 g for 10 min at 4°C. Cell lysates were subjected to SDS-PAGE. Western blots were performed with rabbit antibodies against GAPDH (cat. n°. 5174, Cell Signaling Technology), H4 (cat. n°. 13919S, clone Cell Signaling Technology) and H2A (cat. n°. 2578S, Cell Signaling Technology).

Four-fold concentrated SDS sample buffer was added to cell lysates, heated at 96°C for 7 min, iced for 5 min, subjected to electrophoresis on a 15% SDS-polyacrylamide gel, and then transferred onto a nitrocellulose sheet. Protein molecular weight standards (Bio-Rad) were run concurrently. The sheet was blocked in Tris-buffered saline (TBS) with Tween 20 (0.1%) containing 5% nonfat dry milk for 1 h at room temperature. Then, membranes were incubated overnight at 4 °C with rabbit anti-GAPDH (1:2000), anti-H4 (1:1000), anti-H2A (1:1000). After

washing 3 times with TBST, the membranes were stained with anti-rabbit secondary antibody (1:5000; Merck, AP510P, polyclonal) for 2 h. After washing 3 times with TBS, membranes were incubated with the chemiluminescent substrate (SuperSignal, Thermo Scientific) and imaged with ChemiDoc MP system (Bio-Rad).

Differential gene expression

Gene expression analysis was performed by Real-Time polymerase chain reaction (RT-PCR) after RNA isolation and cDNA synthesis. RNA isolation was performed using the Quick-RNA™ MiniPrep Plus (Zymo Research®), following the manufacturer's instructions. RNAs were stored at −80 °C until cDNA synthesis was performed using the ImProm-II™ Reverse Transcription (Promega®). cDNAs were synthesized using the PTC-100™ Programmable Thermal Controller (MJR/BioRad) thermocycler and stored at −20°C until use.

RT-PCR was performed using Applied Biosystems™ StepOne™ system with Master Mix Syber Green (QuatroG P&D Ltda), following the manufacturer's instructions. The specific primers were synthesized by IDT (Coralveille, Iowa, USA) and listed in Table 1. The expression level of each gene was normalized by *GAPDH* or *β-ACTIN* and expressed as a fold change concerning the control group (undifferentiated THP-1), using the 2-ΔΔCT method [36]. Each sample was quantified in triplicate and points containing nuclease-free water were used as negative controls.

Qualitative PCR

Qualitative PCR was performed using Platinum DreamTaq Green PCR Master mix (Fermentas®) following the manufacturer's instructions, using the primer SK44 (5'-GAGCCGATAA CGCGTCCATCG-3') for HTLV-1 tax. The second round of PCR was performed under the same conditions using 2 µl of the products from the first PCR round. The amplification cycle consisted of enzyme activation at 94 °C for 3 min, 35 cycles of denaturation at 94 °C for 30 s, annealing at 60 °C for 30 s, extension at 72 °C for 30 s, and a final extension step at 72 °C for 10 min. PCR products were electrophoresed in 2% agarose (Sigma-Aldrich/Merck) gel stained with GelRed® (Biotium) in 1× Tris-Borate-EDTA buffer (Invitrogen) at 100 V for 90 min. The bands were visualized using the MiniBis Pro ultraviolet transilluminator (DNR Bio-Imaging Systems Ltd®).

Statistical analysis

Experimental data were analyzed using the Prisma 8.0 Software. The values expressed in the graphs indicate the mean ± standard error of the mean. Statistical analysis was performed using a two-tailed *Student t*-test or

Table 1 Primers used for gene expression by real-time PCR

Primer	Forward	Reverse	[ ]
β-actin	CAGGCACCAGGGCGTGAT	GCCAGCCAGGTCCAGACG	200 nM
Gapdh	GTGAAGGTCGGAGTCAACGG	CTCCTGGAAGATGGTGATGGG	200 nM
TNF-α	TGTAGCAAACCCTCAAGCTG	TTGATGGCAGAGAGGAGGTT	200 nM
TLR-4	CAGAGTTGCTTTCAATGGCATC	AGACTGTAATCAAGAACCTGGAGG	200 nM
IL18	AACAAACTATTTGTCGCAGGAAT	TGCCACAAAGTTGATGCAAT	200 nM
IL6	GCCCAGCTATGAACTCCTTCT	CTTCTCCTGGGGGTACTGG	200 nM
TLR-2	GGGTCATCATCAGCCTCTCC	AGGTCACTGTTGCTAATGTAGGTG	200 nM
IL-1β	TTACAGTGGCAATGAGGATGAC	GTCGGAGATTCGTAGCTGGAT	200 nM
MD-2	GCTCAGAAGCAGTATTGGGTCTG	CGCTTTGGAAGATTCATGGTG	400 nM
ARG1	ACGGAAGAATCAGCCTGGTG	GTCCACGTCTCTCTCAAGCCAA	400 nM
CCL22	ATCGCCTACAGACTGCACTC	GACGGTAACGGACGTAATCAC	200 nM
TGF-β	GCCCTGGACACCAACTATTGC	GCTGCATTGCAGGAGCGCAC	200 nM
ISG15	GCCTCAGCTCTGACACC	CGAACTCATCTTTGCCAGTACA	200 nM
IFN-β	ATGACCAACAAGTCTTCAAAG	GGAATCCAAGCAAGTTGTAGCTC	200 nM
IL-28	TCCAGTCACGGTCAGCA	CAGCCTCAGAGTGTTTCTTCT	200 nM
IL-29	GAAGACAGGAGAGCTGCAAC	GGTTCAAATCTCTGTCACCACA	200 nM
OASL	GCAGAAATTTCCAGGACCAC	CCCATCACGGTCACCATTG	200 nM
H2A	AGCTCAACAAGCTTCTGGGCAA	TTGTGGTGGCTCTCGGTCTTCTT	400 nM
H2B	TGCGCCCAAGAAGGGTTCTAAA	ACGAAGGAGTTCATGATGCCCA	200 nM
H4	ACCGTAAAGTACTGCGCGACAA	TTCTCCAGGAACACCCTTCAGCA	400 nM
H1S4	CCGGTGTCCGAGCTCATTACTAAA	GCTTTCTTGAGAGCGGCCAAAGAT	200 nM

One-way repeated-measures ANOVA with Bonferroni's multiple comparison post-test. Values of $p < 0.05$ were considered significant.

Computational analysis of published transcriptomic datasets

Datasets GSE29312 of Tattermusch et al., 2012, and GSE117040 of Gerrick et al., 2018 were obtained from the Gene Expression Omnibus (GEO) database. The dataset GSE29312 characterizes global gene expression profiles of blood cells taken from AC and HAM/TSP patients by HumanHT-12 V3 or WG6 V3 expression BeadChip arrays (Illumina, San Diego, CA, USA) [37] and the dataset GSE117040 characterized differential gene expression from macrophages derived from human peripheral blood monocytes cultured in the presence of LPS and IFNγ to induce M1 polarization, or IL-4 and IL-13 to induce M2 polarization. The authors used TrueSeq Stranded Total RNA kit (Illumina) to prepare the libraries and sequenced by HS2500 Rapid Run instrument Illumina [38]. Differential gene expression results from both datasets were downloaded using R Studio GEOquery package software [39]. Data were visualized using the R packages ggplot2 and ComplexHeatmap [40, 41].

Results

HTLV-1-infected cells induced macrophage differentiation in vitro

To evaluate the monocyte profile during HTLV-1 infection, we used an in vitro system. The human monocytic cell line (THP-1) was cultured with HTLV-1-infected cells (MT-2), previously irradiated, and THP-1 cell morphology and viability were analyzed after 6 days. The co-culture with MT-2 or PMA did not impact cell viability (Supplementary Figure 1). THP-1 cells showed a non-adherent and rounded morphology of monocytes, as described in the literature (Fig. 1A). PMA stimulation was used as a positive control for macrophage differentiation [33]. Interestingly, cells co-cultured with MT-2 spread out and adhered to the plate surface, acquiring a macrophage-like morphology, as also observed for PMA-treated cells (Fig. 1A). Moreover, THP-1 cells cultured with MT-2 expressed CD68, a surface marker highly

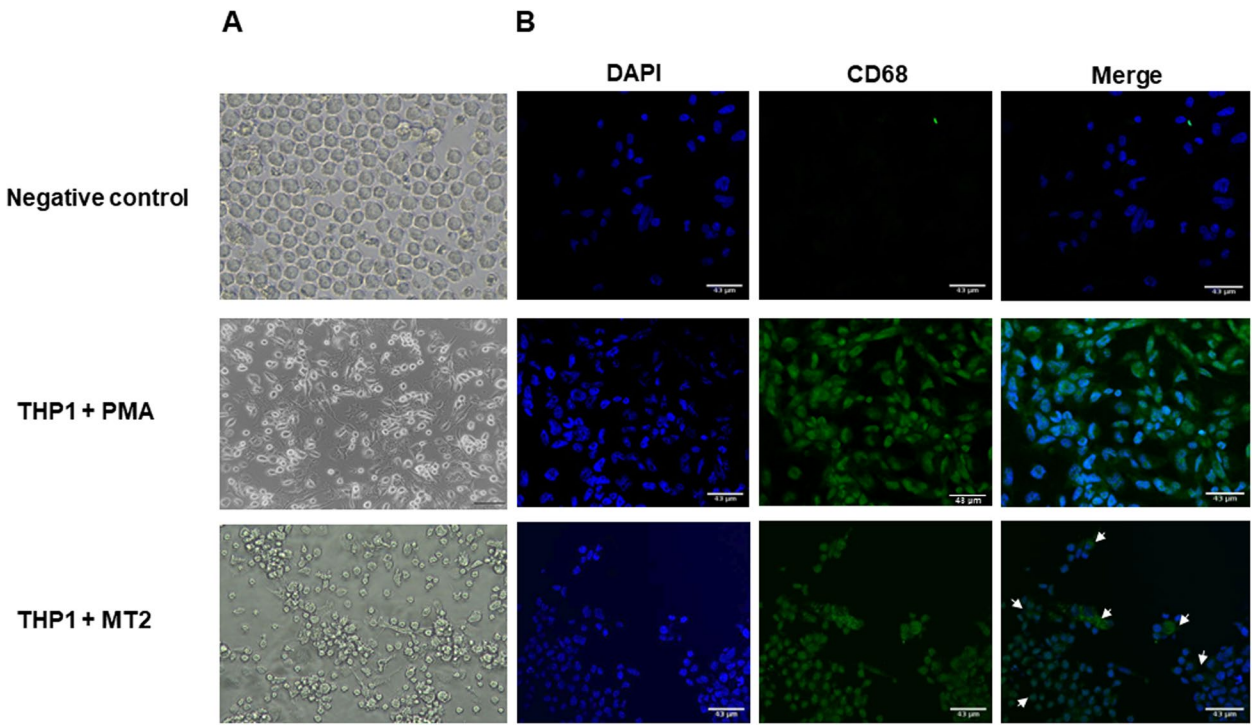

Fig. 1 Analysis of morphology and CD68 expression in THP-1 cells co-cultured HTLV-1-infected cells (MT-2). THP-1 monocytes were incubated in 24-well plates with coverslips for 6 days. Monocytes were co-cultured with HTLV-1-infected cells (MT-2 irradiated at 20 Gy) in a 1:2 ratio. Cells treated with PMA (100 nM) or untreated were used as controls, positive and negative, respectively. **A** On day 6, cell morphology was analyzed by phase contrast microscopy in 20x magnification objective, using a light microscope (Olympus CKX41). **B** Macrophage phenotype was characterized using CD68 in immunofluorescence assay. After the THP1 culture, cells were permeabilized and stained with intracellular antibody CD68 FITC, followed by nucleic acid staining with DAPI. CD68-positive cells were indicated with white arrows. Photographs were taken on a Leica® fluorescence microscope at 40x magnification, and images were analyzed in ImageJ Software

expressed in macrophages (Fig. 1B and supplementary Figure 2). These results suggested monocyte differentiation into macrophages in the presence of HTLV-1-infected cells.

To further evaluate the differentiation, we explored prototypical macrophage surface molecules. The levels of HLA-DR, a class II MHC molecule, increased in THP-1 cells after co-culture with MT-2 (Fig. 2A and supplementary Figure 3). The mean fluorescence intensity (MFI) was approximately 50-fold higher compared to undifferentiated cells (THP-1 CTR; Fig. 2A). Co-stimulatory molecules CD80 and CD86 also increased significantly (Fig. 2B-C). More than 50% of cells cultured with MT-2 cells expressed CD86. It was approximately 200-fold higher than THP-1 CTR (Fig. 2C). No difference was observed in the frequency of cells expressing CD14 (Fig. 2D) but both THP-1 co-cultured with MT-2 and treated with PMA expressed higher levels of CD14, as demonstrated by the MFI in Fig. 2D. The frequency of $CD32^{+}$ (Fcγ receptor II) cells and their MFI were slightly increased after co-culturing with MT-2 or PMA (Fig. 2E). We also observed an increase in the levels (MFI) of $CD127^{+}$ (IL-7α receptor) cells after the co-culture compared to the undifferentiated THP-1 (CTR) (Fig. 2F). Altogether these results support the hypothesis that monocyte differentiation into macrophages is induced by the HTLV-1-infected cells.

THP-1 cells co-cultured with HTLV-1-infected cells express high levels of pro-inflammatory genes

Monocyte-derived macrophages can polarize into different populations, usually M1 (classic) and M2 (alternative) [42]. Given that HTLV-1-infected cells induce changes in the THP-1 phenotype, we evaluated the expression of M1 and M2-associated genes after co-culturing with MT-2. The mRNA levels for pro-inflammatory cytokines TNF-α, IL-6, and IL-1β were upregulated in THP-1 cells (Fig. 3A). THP-1 macrophages differentiated using PMA and stimulated with LPS for 24 h were used as a positive control and showed upregulation of pro-inflammatory genes (Supplementary Figure 4). Similarly, higher concentrations of TNF-α and IL-6 were found in the supernatant of THP-1 co-cultured with MT-2 (Fig. 3B). Members of the matrix metalloproteinase (MMP) family are highly observed in various inflamed tissues [43] and MMP1 is an indicator of PMA-induced THP-1 cell differentiation [44]. MMP-1 was increased in PMA-differentiated cells (4370 ± 725.5 pg/mL) compared to control cells (320.4 ± 320 pg/mL; Fig. 3C). After co-culture with MT-2, MMP-1 also increased (1024 ± 615.1 pg/mL), but the presence of MT-2 in the culture induced a higher production of MMP-2 (Fig. 3C). Furthermore, soluble CD14 (sCD14) was highly produced after co-culturing compared to undifferentiated cells (Fig. 3D), and manner consistent with the high expression of *TLR2* and *TLR4* (Fig. 3E).

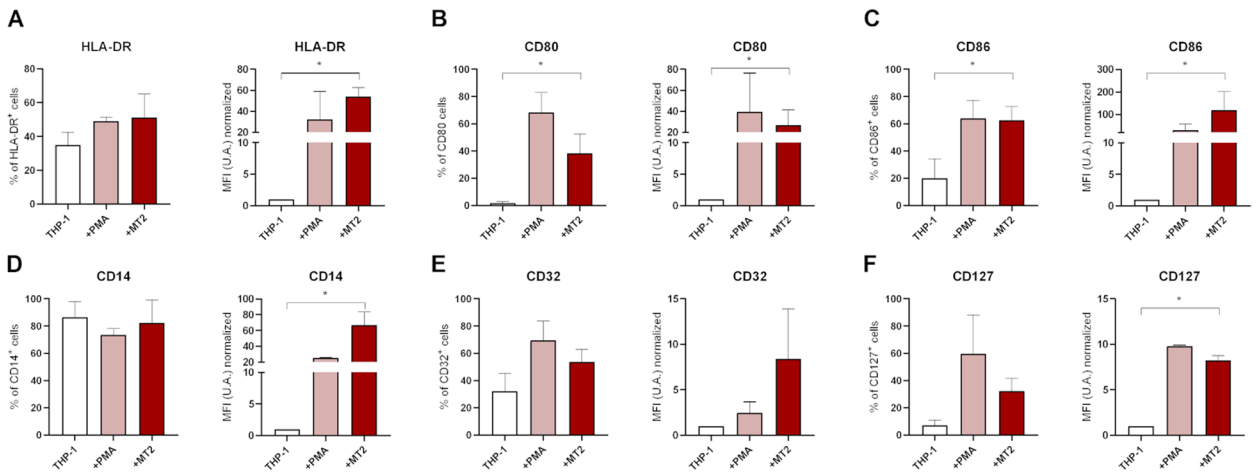

Fig. 2 Analysis of surface molecules in THP-1 cells co-cultured with MT-2. THP-1 cells were co-cultured with MT-2 (irradiated at 20 Gy) in a 1:2 ratio or treated with PMA (100 nM, positive control) for 6 days. On day 6, differentiated cells were detached with PSB + EDTA (100 nM) and stained with antibodies for flow cytometry. Frequency and media fluorescence intensity (MFI) of **A** HLA-DR, **B** CD80, **C** CD86, **D** CD14, **E** CD32, and **F** CD127 in THP-1 cells cultured alone (THP-1), stimulated with PMA (+ PMA) or co-cultured with MT-2 (+ MT-2). Means of MFI were normalized based on the expression pattern of undifferentiated THP-1 control cells. Graphs are mean ± SEM values from 3 to 5 independently performed experiments. *$p < 0.05$ compared to controls (THP-1)

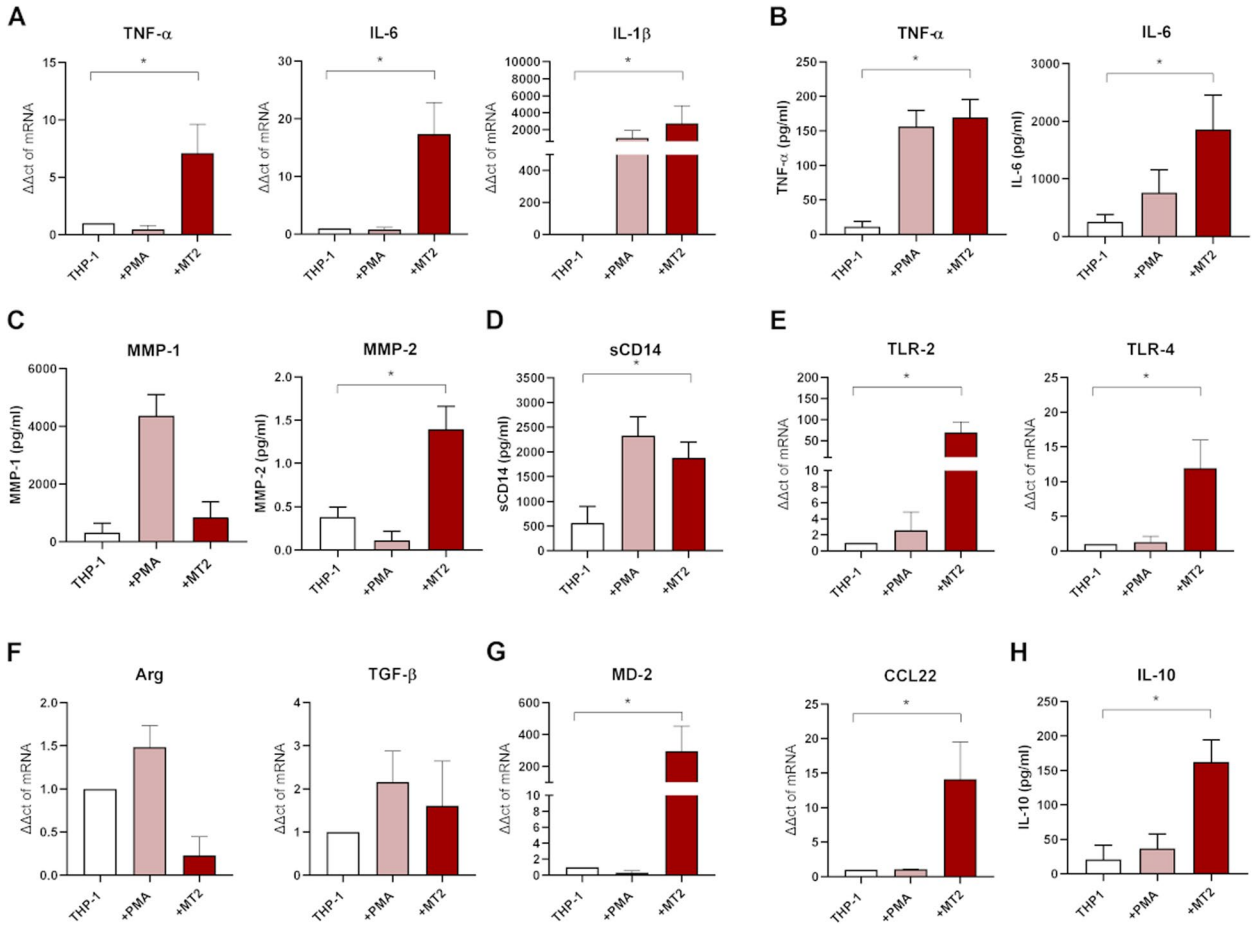

Fig. 3 Analysis of gene expression and cytokines associated with M1-M2 profile in cells co-cultured with MT-2. THP-1 cells were co-cultured with MT-2 (irradiated at 20 Gy) in a 1:2 ratio or treated with PMA (100 nM, positive control) for 6 days. On the sixth day, cells were lysed for RNA extraction and cDNA synthesis for RT-PCR, and cultured supernatants were collected to mediators were assayed by the ELISA method. mRNA expression of M1-associated pro-inflammatory genes **A** TNF-α, IL-6, IL-1, **E** TLR-2, and TLR-4; **F** and **G** mRNA expression of M2-associated genes Arg, TGF-β, CCL22, and MD-2. Graphs represent relative mRNA levels, calculated using the 2-ΔΔCT method and normalized to Gapdh or β-actin in the same sample, compared to the expression of the respective genes in undifferentiated THP-1 cells. **B** Detection of TNF-α, IL-6, **D** sCD14, **C** MMP-1 and MMP-2, **H** IL-10, concentration in cultured supernatant. Graphs are mean ± SEM values of supernatants from 4 to 7 independently performed experiments. *$p < 0.05$ compared to controls (THP-1)

Regarding M2-associated genes, we did not observe upregulation of arginase (*ARG*) or TGF-β (Fig. 3F). Dexamethasone-treated cells were used as a positive control for M2 differentiation (Supplementary Figure 4). Interestingly, *MD2* and *CCL22* were induced by the co-culture with MT-2 (Fig. 3G) as well as the release of IL-10 in the supernatant (Fig. 3H). These data suggest the induction of a profile associated with M1 polarization in THP-1 cells co-cultured with HTLV-1-infected cells predominantly.

High levels of interferon-stimulated genes were induced in THP-1 cells after co-culture with MT-2

Antiviral responses are characterized by the upregulation of Interferon-Stimulated Genes (ISGs) [45]. We accessed the expression of some genes of the interferon family (IL-18, IL-28, IL-29, and IFN-β), and ISGs (OASL and ISG15). THP-1 cells co-cultured with MT-2 showed significant upregulation of IL-29, IFN-β, OASL, and ISG15 genes (Fig. 4A and Supplementary Figure 5). Moreover, THP-1 cells co-cultured with MT-2 secreted higher levels of CXCL10, chemokine stimulated by IFN (Fig. 4B). Positive controls are represented in supplementary Figure 4. Lee et al., 2019 demonstrated that tryptophanyl-tRNA synthetase (WARS) is induced and released during viral infection [46]. This enzyme acts as an alarmin and stimulates type I IFNs production and mutations in *WARS* gene have been associated with motor neuropathy [47, 48]. Figure 4C shows the upregulation of *WARS* in THP-1 cultured with MT-2.

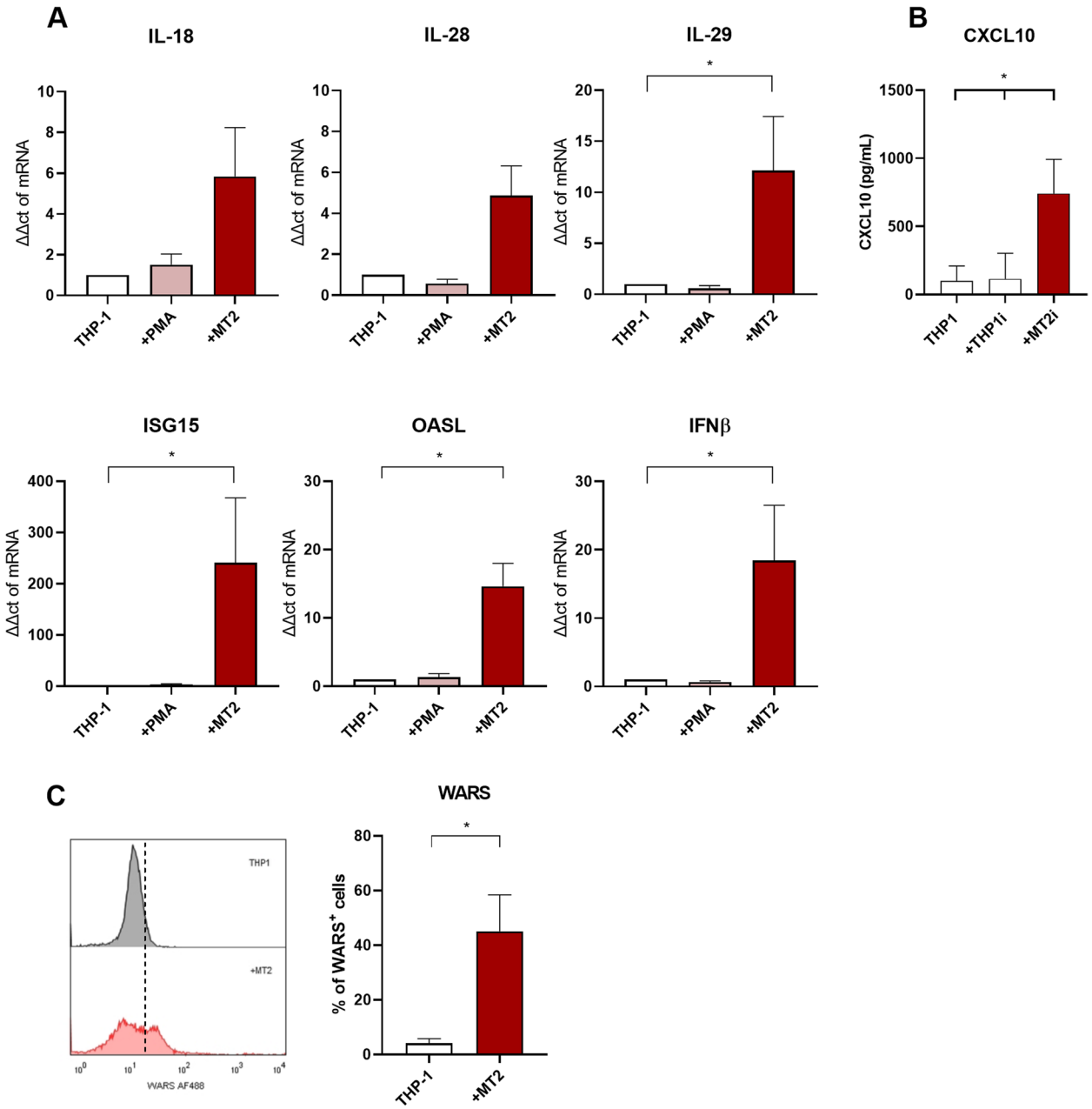

Fig. 4 Analysis of gene expression associated with the IFN response in THP-1 cells co-cultured with MT-2. THP-1 cells were co-cultured with MT-2 (irradiated at 20 Gy) in a 1:2 ratio or treated with PMA (100 nM, positive control) for 6 days. After that, cells were lysed for RNA extraction and cDNA synthesis for RT-PCR. **A** mRNA expression of IL-18, IL-28, IL-29, ISG15, OASL, and IFN-β. Graphs represent relative mRNA levels from 4 independently compiled experiments, calculated using the 2-ΔΔCT method and normalized to Gapdh or β-actin in the same sample, compared to the expression of the respective genes in undifferentiated THP-1 cells. **B** Detection of CXCL10 concentration in cultured supernatant performed by ELISA. Graphs are mean ± SEM values of supernatants from 3 independently performed experiments. *$p < 0.05$ compared to controls (THP-1). **C** After the co-cultures, the WARS expression was investigated by flow cytometry, using a specific polyclonal antibody. The values on the graphs are mean ± SEM values of supernatants from 4 independently performed experiments. *$p < 0.05$ compared to controls (THP-1)

HTLV-1 infection reduced histone genes transcription in THP-1 macrophages

HTLV-1-infected cells undergo epigenetic modifications [49, 50]. Moreover, our group demonstrated a negative regulation of histone expression in monocytes of HTLV-1 carriers through proteomic analyses [17]. We sought to investigate whether the co-culture of THP-1 with MT-2 affects the expression of histones. The mRNA expression

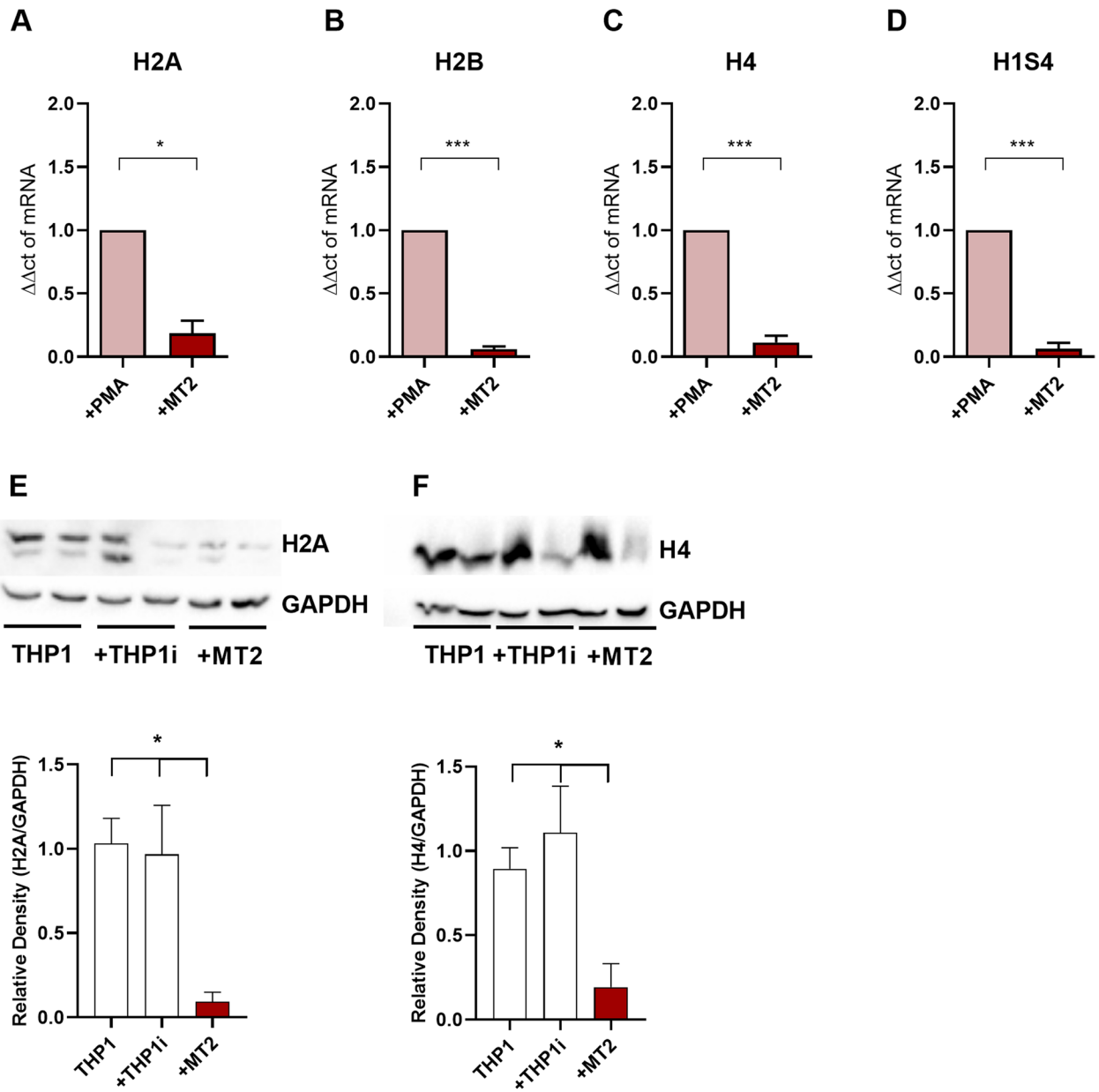

Fig. 5 Analysis of histone gene expression in THP-1 cells co-cultured with MT-2. THP-1 cells were co-cultured with MT-2 (irradiated at 20 Gy) in a 1:2 ratio or treated with PMA (100 nM, positive control) for 6 days. After that, cells were lysed for RNA extraction and cDNA synthesis for RT-PCR. **A** mRNA expression of H2A, **B** H2B, **C** H4 and **D** H1S4. Graphs represent relative mRNA levels from 4 independently compiled experiments, calculated using the 2-ΔΔCT method and normalized to Gapdh in the same sample, compared to the expression of the respective genes in undifferentiated THP-1 cells. The values on the graphs are mean ± SEM values of supernatants from 3–4 independently performed experiments. *$p < 0.01$ and ***$p < 0.0005$ compared to PMA. 20 µL of total proteins from THP1, THP1 + THP1 irradiated cells (+THP1i), and THP1 + MT-2 irradiated cells (+MT-2) from 3 independent culture experiments. The protein extracts were separated in SDS-PAGE and transferred to nitrocellulose membrane to analyze **E** H2A and **F** H4 content by western blot using GAPDH as a constitutive protein as described above. Relative densitometry of H2A and H4 in relation to GAPDH was performed using ImageJ software. This is a representative figure from 2 independent experiments performed in duplicates. Full uncropped gels from Western Blot gels in supplementary Figures 6–8

of H2A, H2B, H4, and H1S4 is downregulated in THP-1 cells co-cultured with MT-2 (Fig. 5A-D). These results were confirmed by western blot assay. Protein levels of H2A and H4 histones were reduced in THP1 monocytes co-cultured with MT-2 comparing control groups (Fig. 5E-F), suggesting that the macrophage differentiation induced by HTLV-1-infected cells affects histone gene expression.

THP-1 co-cultured with MT-2 cells or its supernatant-induced cellular alterations and infection

The fact that THP-1 acquired an M1-like phenotype conducted the hypothesis that MT-2 lymphocytes might be contacting THP-1 monocytes, inducing its activation and differentiation to macrophages. To address this hypothesis, THP-1 monocytes and MT-2 cells were co-cultured with MT-2-filtered supernatant (SN MT2), or an insert to block cell contact. Co-cultured cells with MT-2 supernatant still induce

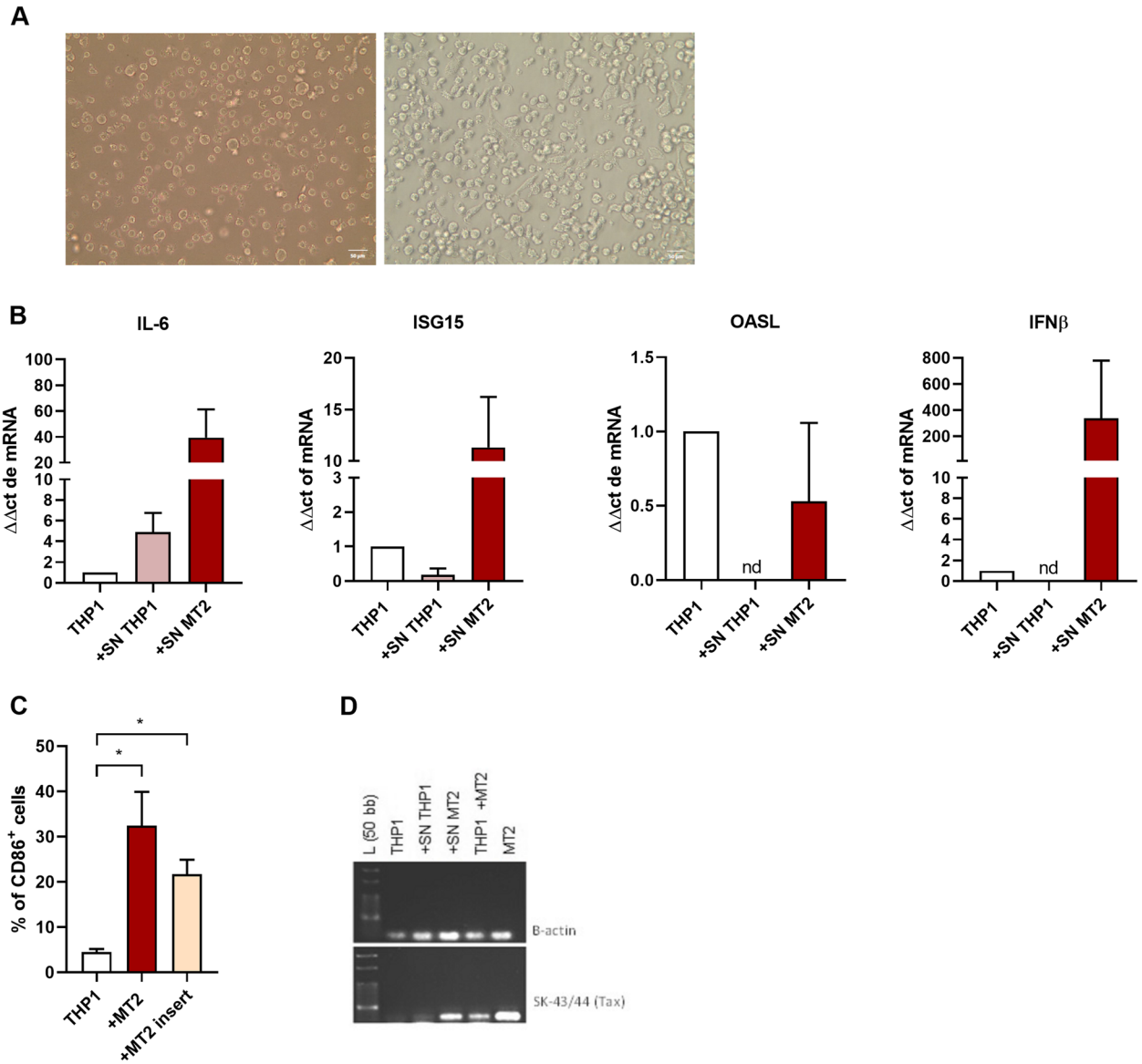

Fig. 6 Analysis of gene expression by THP-1 cells co-cultured with MT-2 cells or their supernatant. THP-1 and MT-2 cells were cultured for 3 days at 37ºC for supernatant isolation. Then, fresh THP-1 cells were co-cultured with or without supernatants from THP1 or MT-2 cells. After 6 days, the morphology of these cells was analyzed by contrast phase microscopy. **A** Representative picture of cells. Photographs were taken on a Leica® fluorescence microscope at 40x magnification, and images were analyzed in ImageJ Software. Representative graph of 2 or 3 independently compiled experiments. After the culture, cells were lysed for RNA extraction and cDNA synthesis to perform RT-PCR (**B**) mRNA expression of IFN-β, OASL, ISG15, and IL-6. Representative image of 3 independently performed experiments. Nd = not detected. *$p < 0.05$ compared to controls (THP1). THP1 cells were also cultured in the presence of MT-2 without cell contact, using an insert as described in the methods. Following, cells were stained and analyzed by flow cytometry. **C** Percentage of $CD86^+$ cells. **D** PCR was used to detect a fragment of 159-bp of HTLV-1 tax in DNA samples obtained from THP1 cells (uninfected control); + SN THP1 (THP-1 cells cultivated with THP1 supernatant); + SN MT-2 (THP-1 cells cultivated with MT-2 supernatant); THP1 + MT-2 (culture of THP-1 in presence of MT-2 cells); MT-2 (DNA from MT-2 cells, used as positive control). The β-actin gene was used as a constitutive control. L – 50-bp DNA ladder

monocyte differentiation (Fig. 6A). Pro-inflammatory cytokine IL-6 and ISGs, such as ISG15, OASL, and IFN-β were upregulated in THP-1 cells co-cultured with MT-2 supernatant (Fig. 6B). Furthermore, the frequency of $CD86^{+}$ cells increased after co-culture without cell contact (Fig. 6C). These data suggested that products secreted by MT-2 can induce THP-1 differentiation and activation of genes related to the inflammatory and antiviral response.

HTLV-1 infects monocytes and macrophages [16, 18]. We next investigated whether THP-1 is infected with HTLV-1, demonstrated by the expression of *tax* (SK43/44), after co-cultivation with MT-2 cell or its supernatant. This gene was found in THP-1 after the co-culture with MT-2 cells (THP-1 + MT-2) and MT-2 supernatant (+ SN MT-2; Fig. 6D). These findings indicate that the presence of HTLV-1-infected cells in the culture is enough to induce monocyte activation and differentiation into M1-like macrophages. The cellular changes observed in the present study may be related to the infection of THP-1 cells, including a non-cell contact-dependent manner.

Signatures of macrophages and their subpopulations in HTLV-1 patients

Changes in phenotypic and functional profiles of monocytes from people living with HTLV-1 have been demonstrated by our group [16, 17] and others [51]. Our in vitro findings demonstrated that HTLV-1 induces macrophage differentiation in an inflammatory profile, predominantly, but also expressing suppressor genes. To evaluate whether this phenotype is observed in HTLV-1 human carriers and further investigate monocytes and macrophages phenotypic and molecular profile, we compared PBMC gene expression data published by Tattermusch et al., 2012 (GSE29312) [37] with M1/M2 transcriptional profiles from Gerrick et al., 2018 (GSE117040) [38]. 51 genes were commonly expressed on "M1" and "HTLV-1" transcriptional signatures (Fig. 7A-C, supplementary Table 1), including genes associated with type 1 interferon (*CCR7*, *IL23*, *IFITM3*, *WARS*) and purinergic receptors (*P2RY2*, *P2RY14*). In contrast, 52 genes were both upregulated in "M2" and "HTLV-1" signatures such as *F13A1* (related to coagulation), *CASP5* (regulation of the inflammatory response), *DNSE1L3* (apoptotic cell

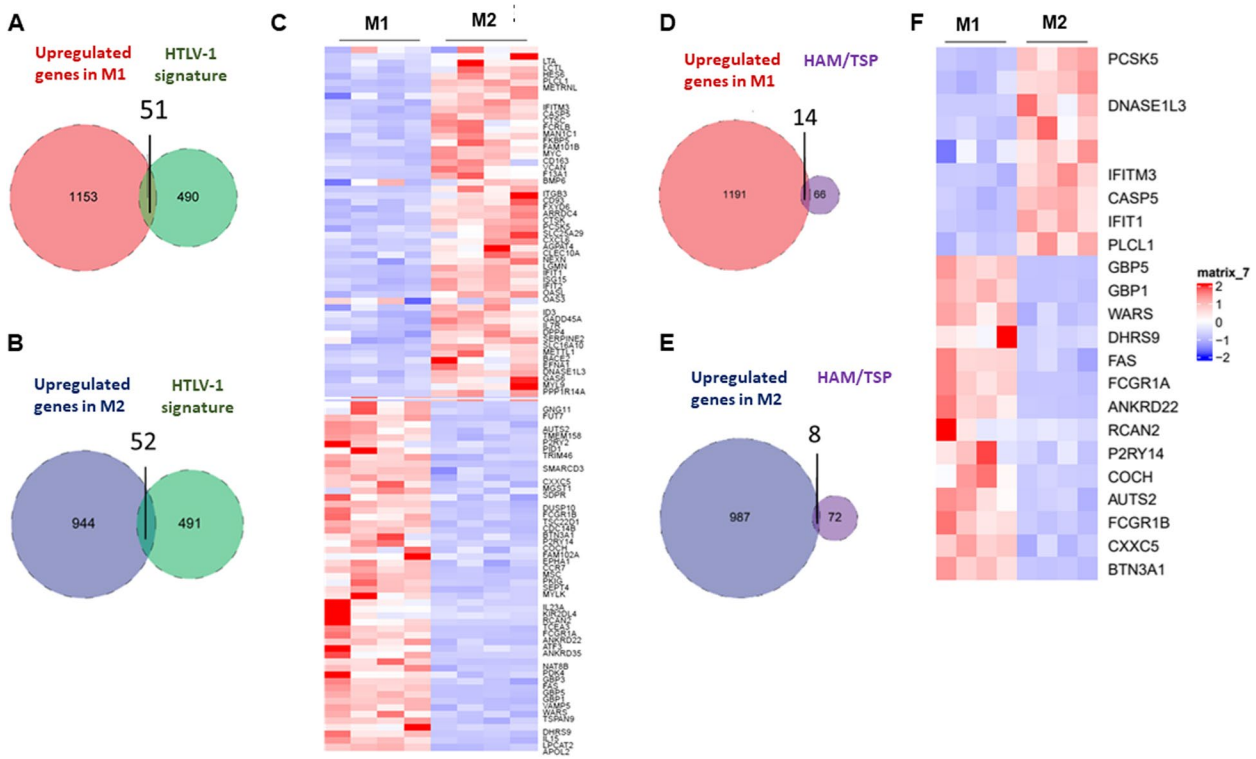

Fig. 7 Correlation between M1/M2 macrophage transcriptional profile and HTLV-1 or HAM/TSP transcriptional signatures. Datasets were obtained from Gerrick et al. [38] and Tattermusch et al. [37] publications (GSE117040 and GSE29312, respectively). Venn diagrams comparing the intersection of M1- or M2-associated genes (1205 and 995, respectively) macrophage with **A-B** HTLV-1 (542 genes) or **D-E** HAM/TSP (80 genes) signatures; **C**; **F** Heatmap of M1 and M2 macrophage subpopulations during HTLV-1 infection (**C**) and HAM/TSP (**F**) normalized by Z score. Data were visualized in Heatmaps and Venn diagrams, using the R packages ggplot2, Complex Heatmap, and Venn Diagram. M1 ∩ HTLV-1: $p = 0.000020577$; M2 ∩ HTLV-1: $p = 0.0000022564$; M1 ∩ HAM/TSP: $p = 0.0001048$; M2 ∩ HAM/TSP: $p = 0.01893$

death) and *CTSC* (antigen processing). Interestingly, the ISGs *IFIT1/2*, *OASL/3*, and *IFITM3* were upregulated on the "M2" signature (Fig. 7C) and were similarly found in THP-1 cultured with MT-2.

We also compared "M1" and "M2"-associated genes with HAM/TSP signature. Figure 7D shows 14 genes in the intersection of "M1" and "HAM/TSP". Genes associated with antiviral response (*GBP1*, *WARS*, *BTN3A1*, *IFITM3*, and *GBP5*) were commonly expressed, as well as purinergic receptors (*P2RY2* and *P2RY14*) and cell death (FAS) genes (Fig. 7F). The "M2" and "HAM/TSP" also exhibited 8 genes commonly expressed (Fig. 7E), related to neurodegeneration (*BACE2*), antiviral response (*GBP5*, *CASP5*, *GBP1*, *IFIT1*, and *IFITM3*), and signal transduction (*PLCL1*). We presuppose that its upregulation contributes to neuroinflammation and antiviral response.

Discussion

It is well described that HAM/TSP development and progression involve mononuclear cells, including monocytes and macrophages [17, 21, 52]. Given the difficulty of obtaining animal models to study HTLV-1, we used an in vitro model to characterize monocyte differentiation during the HTLV-1 infection.

In this study, we demonstrated that HTLV-1-infected cells induced THP-1 monocyte activation and differentiation into macrophages. THP-1 cells acquired a macrophage morphology, up-regulated the levels of surface molecules (HLA-DR, CD80, CD86, CD14, CD127, TLR4, and TLR2), and increased the expression and/or levels of inflammatory cytokines (IL-6, TNF-α, IL-1β) and MMP2. Surprisingly, the upregulation of M2-associated molecules, such as *CCL22*, *IL-10*, and *MD-2* was observed after the co-culture. Moreover, the monocyte interaction with HTLV-1-infected cells resulted in a cellular antiviral state characterized by ISGs expression (*IFN-β*, *IL-29*, *OASL*, and *WARS*). We showed that HTLV-1-infected cells can induce macrophage differentiation and infection regardless of cell contact.

We can attribute these findings, at least partially, to viral infection. After co-culture THP1 monocytes were infected, suggesting virus infection participation in THP1 differentiation. Corroborating this result many studies showed HTLV-1 infection in monocytes and macrophages [14–18, 53]. The differentiation can be induced by cytokines secreted from MT-2 cells. These cells can produce TNFα, IL-6, IL-1α, IL-17, and IFNγ [54, 55]. To clarify the role of HTLV-1 infection in monocyte differentiation to macrophage cell transfection assays could be used, eliminating the participation of secreted molecules. These results suggested that the mechanisms of THP1 differentiation depend on cytokines, metabolites, and viral proteins as Tax secretion. Besides the direct Tax production by infected cells, viral protein is transferred by cell contact and/or exosomes [56, 57]. Tax protein activates several specific transcription factors such as CREB (cAMP response element binding protein), AP-1, NF-κB, JNK, IRF4, and mTOR [58–60]. The hyperactivation of some of these factors was associated with macrophage M1 polarization during bacterial or viral infection [61]. Tax protein participates in viral replication, leading to histone ubiquitylation, which can be related to epigenetic modifications (methylation) and protein degradation [62–64]. Moreover, Grant et al. (2006) suggested that infected-monocyte AP-1 expression is up-regulated during differentiation to macrophages [65]. According to our results, this phenomenon may mean a greater differentiation capacity for macrophages. After co-culture THP1 monocytes presented a reduction in the levels of mRNAs (*H2A*, *H2B*, *H4*, *H1S4*) and protein (H2A and H4) for histones, suggesting an effect on chromatin regulation. Interestingly, our group has demonstrated a reduction of histone expression in monocytes obtained from HTLV-1-infected individuals, using proteomic and immunofluorescence assays [17]. Furthermore, epigenetic modifications, such as hypomethylation and hypermethylation in H3K4 and H3K27, have been demonstrated during human monocyte differentiation to macrophage [66].

To further understand monocyte and macrophage profile during the infection and complement our findings, we compared M1 and M2 macrophage transcriptional gene signatures with signatures from PBMCs of HTLV-1-infected donors, including HAM/TSP patients. Common expression of several genes was remarkable: while the M1 signature in asymptomatic infection was marked by genes associated with inflammation, antigen processing, and antiviral response; the M2 signature was highlighted by associated genes with coagulation, apoptosis, and regulation of immune response. Interferon-inducible genes *IFITM3*, *WARS*, *GBP1*, *GBP5*, *CCR7*, *ISG15*, and *OASL* were likewise in the intersection of macrophages (M1 and M2) and HTLV-1 or HAM/TSP gene signatures supporting our in vitro findings.

Zarei Ghobadi et al. (2020) analyzed three microarray datasets to identify gene transcriptional signatures associated with HAM/TSP development, which we used to associate our data and found an intersection. The authors found 38 modules enriched in HAM/TSP patient signatures [67], including the IL-10 signaling pathway, associated with M2 phenotype, and cytokine detected in this work. The involvement of immunological-related proteins, PSME1 and GBP5, can be considered an intersection of both findings. The proteasome is an important component of the processing by class I MHC peptides composed of core and regulator complexes. The PSME1

(or proteasome activator subunit 1) is an immunoproteasome component connected to class I MHC peptide processing [67]. IFNγ induces the gene encoding PSME1 [68], like HLA-DR, CD80, and CD86 [69]. These molecules are upregulated for effective antigen presentation during APC maturation [70, 71]. The PSME1 was associated with HAM/TSP progression [67], and we connected this data to HLA-DR, CD80, and CD86 upregulation after THP1 monocytes co-cultured with HTLV-1-infected cells due to common related functions. Moreover, these proteins were also related to M1 polarization during the attenuated strain of Junin virus (etiological agent of Argentine hemorrhagic fever) [72]. In addition, GBP5 protein (guanine nucleotide-binding protein 5) was also detected in the comparison of published datasets and can be associated with M1 macrophage polarization due to its effects. This GTPase was induced by influenza A virus infection, then stimulated infected-cell antiviral state, leading to IFNs type I and III expression genes [73]. Corroborating our data, it is known that GBP5 also promotes ISGs activation and proinflammatory cytokines production such as TNF-α, IL-6, and IL-1β/IL-18 [74, 75]. Additionally, higher levels of IL-18 in cerebrospinal fluid from HAM/TSP patients have been demonstrated and validate this enhancement to neuroinflammation and BBB disruption [75].

Macrophage polarization has been classified on a transcriptional level to describe tissue-specific states. A significant macrophage diversity has been observed in morphology, function, and cell surface molecule expression [76]. Altogether, our findings propose the ability of monocyte differentiation into macrophages that may contribute to pro-inflammatory and anti-viral responses observed by the upregulation of associated genes. Although few features of M2 macrophages are still found during the infection, we suggest that the M1 phenotype may contribute to HAM/TSP progression based on Zarei Ghobadi et al. (2020) findings [67]. However, more specific studies are needed to further understand the role of M1 and M2 macrophages and molecular modifications resulting from HTLV-1 infection.

Abbreviations

HTLV-1	Human T-cell lymphotropic virus type 1
HAM/TSP	HTLV-1-associated myelopathy/tropical spastic paraparesis
AC	Asymptomatic carriers
cDNA	Complementary DNA
CCL	Chemokine (C-C motif) ligand
CCR5	C-C motif chemokine receptor 5
CXCR3	C-X-C motif chemokine receptor 3
CX3CR1	C-X3-C motif chemokine receptor 1
CD	Cluster of differentiation
DC	Dendritic cell
DNA	Deoxyribonucleic acid
GM-CSF	Granulocyte-macrophage colony-stimulating factor
GO	Gene Ontology
HIV-1	Human Immunodeficiency Virus type 1
IFN-γ	Interferon-gamma
IL	Interleukin
ISGs	Interferon-stimulated genes
MD2	Myeloid differentiation protein 2
MFI	Mean fluorescence intensity
ORF	Open reading frame
PBMC	Peripheral blood mononuclear cells
PBS	Phosphate buffered saline
PCR	Polymerase chain reaction
PMA	Phorbol 12-myristate-13-acetate
RNA	Ribonucleic acid
RT-PCR	Real-time PCR
TNF-α	Tumor necrosis factor-alpha

Supplementary Information

The online version contains supplementary material available at https://doi.org/10.1186/s12865-024-00670-8.

Supplementary Material: Supplementary Figure 1. Cell viability analysis of THP-1 cells co-cultured with HTLV-1-infected cells (MT-2). THP-1 monocytes were co-cultured with HTLV-1-infected cells (MT-2 irradiated at 20 Gy) in a 1:2 ratio. Cells treated with PMA (100 nM) as used as controls, positive and negative, respectively. (A) Cell viability analyzed by LDH assay, using supernatants of cultures. (B) On day 6 at 37 ºC in a humid atmosphere with 5% CO_2, cells were stimulated with or without LPS (10 ng/ml) for 24 h and incubated with MTT (5 mg/mL) for 3 h. Colorimetric analysis was measured at 490 nm, using a microplate spectrophotometer reader. Graphs are mean ± SEM values of supernatants from 3 independent experiments performed in duplicates. Supplementary Figure 2. CD68 expression analysis in THP-1 cells co-cultured HTLV-1-infected cells (MT-2). THP-1 monocytes were incubated in 24-well plates with coverslips for 6 days. Monocytes were co-cultured with HTLV-1-infected cells (MT-2 irradiated at 20 Gy) or THP-1 irradiated cells in a 1:2 ratio. Irradiated THP-1 cells were used as a control. On day 6, the macrophage phenotype was characterized using CD68 immunofluorescence assay. After the THP1 culture, cells were permeabilized and stained with intracellular antibody CD68 FITC, followed by nucleic acid staining with DAPI. CD68-positive cells were indicated with white arrows. Photographs were taken on a Nikon Eclipse Ti2 fluorescence microscope at 63x magnification, and images were analyzed in ImageJ Software. Supplementary Figure 3. Flow cytometry gating strategies related to Fig. 2. THP-1 monocytes were co-cultured with HTLV-1-infected cells (MT-2 irradiated at 20 Gy) in a 1:2 ratio. Cells treated with PMA (100 nM) as used as controls, positive and negative, respectively. On day 6, differentiated cells were detached with PSB + EDTA (100 nM) and stained with antibodies for flow cytometry. Gating strategies on cells for immunophenotyping (HLA-DR, CD80, CD86, CD14, CD32, and CD127). All histograms were compared with unstained cells (Negative) using FlowJo Software 10.0. Supplementary Figure 4. analysis of pro-inflammatory mediators produced by THP-1 cells differentiated with PMA. THP-1 cells were treated with PMA (100 nM) for 6 days. On day 6, cells were stimulated with LPS (10 ng/ml; M1 positive control) for 24 h or dexamethasone (100 nM; M2 positive control) for 72 h. Following, cells were lysed for RNA extraction and cDNA synthesis for RT-PCR. mRNA expression of TNF-α, IL-6, IL-1β, TLR2, TLR4 after LPS stimuli; mRNA expression of Arg, MD2, CCL22, TGFβ after LPS and/or dexamethasone treatment. Graphs represent relative mRNA level, calculated using the 2-ΔΔCT method and normalized to Gapdh or β-actin in the same sample, compared to the expression of the respective genes in PMA-treated THP-1 cells. Supplementary Figure 5. analysis of ISGs expression by THP-1 cells differentiated with PMA. THP-1 cells were treated with PMA (100 nM) for 6 days. On day 6, cells were stimulated with LPS (10 ng/ml; M1 positive control) for 24 h or dexamethasone (100 nM; M2 positive control) for 72 h. After LPS and/or dexamethasone treatment, cells were lysed for RNA extraction and cDNA synthesis for RT-PCR. IL-18, IL-28, IL-29, ISG15, OASL, and IFNβ mRNA expression. Graphs represent relative mRNA level, calculated using the 2-ΔΔCT method and normalized to Gapdh or β-actin in the same sample, compared to the expression of the respective genes in PMA-treated THP-1 cells. Supplementary Figure 6. Full uncropped gels from GAPDH western blot gel. The protein extracts were separated into polyacrylamide gels.

Supplementary Figure 7. Full uncropped gels from H2A western blot gel. The protein extracts were separated into polyacrylamide gel. Supplementary Figure 8. Full uncropped gels from H4 western blot gel. The protein extracts were separated into polyacrylamide gel.

Acknowledgements
We are thankful to the Flow Cytometry Unit from the Programa de Pós-graduação em Imunologia e Inflamação at the Universidade Federal do Rio de Janeiro. We are thankful to Dr. Andreza Gama for her technical support.

Authors' contributions
S.P.M. S. performed the experiments, data analysis, and writing the original draft; C.C. performed the experiments and the computational analysis; G. A. M. performed the computational analysis and figure elaboration, M. C. S. C., J. V. P., and F. F. D. performed the review experiments R. M. P. and J. E.-L. conceived and designed the experiments edited and reviewed the manuscript text.

Funding
This work was supported by grants from Fundação Carlos Chagas Filho de Amparo à Pesquisa do Estado do Rio de Janeiro (FAPERJ, E-26/211.003/2019), Conselho Nacional de Desenvolvimento Científico e Tecnológico (CNPq). Sabrina Pires Maciel, Guilherme A. Melo, Carolina Calôba, and Maria Clara Salgado Campos were recipients of Fellowships from Coordenação de Aperfeiçoamento de Pessoal de Nível Superior (CAPES). Juliana Vieira Pimenta was a Scientific Initiation scholarship recipient of Conselho Nacional de Desenvolvimento Científico e Tecnológico (CNPq).

Data availability
The original contributions presented in the study are included in the article, further inquiries can be directed to the corresponding author.

Declarations

Ethics approval and consent to participate
Not applicable.

Consent for publication
Not applicable.

Competing interests
The authors declare no competing interests.

Author details
[1]Laboratório de Imunologia Básica e Aplicada, Instituto de Microbiologia Paulo de Góes, Universidade Federal do Rio de Janeiro, Rio de Janeiro, RJ CEP 21941-590, Brazil. [2]Laboratório de Imunologia Molecular, Instituto de Microbiologia Paulo de Góes, Universidade Federal do Rio de Janeiro, Rio de Janeiro, RJ CEP 21941-590, Brazil. [3]Laboratório de Imunologia e Inflamação, Instituto de Microbiologia Paulo de Góes, Universidade Federal do Rio de Janeiro, Rio de Janeiro, RJ CEP 21941- 590, Brazil. [4]Instituto de Microbiologia Paulo de Góes, CCS, Sala I-43, UFRJ, Rio de Janeiro CEP 21941-590, Brazil.

Received: 2 May 2024 Accepted: 14 November 2024
Published online: 20 March 2025

References

1. Gessain A, Barin F, Vernant JC, et al. Antibodies to human T-lymphotropic virus type-I in patients with tropical spastic paraparesis. Lancet. 1985;2(8452):407–10. https://doi.org/10.1016/s0140-6736(85)92734-5.
2. Poiesz BJ, Ruscetti FW, Gazdar AF, Bunn PA, Minna JD, Gallo RC. Detection and isolation of type C retrovirus particles from fresh and cultured lymphocytes of a patient with cutaneous T-cell lymphoma. Proc Natl Acad Sci U S A. 1980;77(12):7415–9. https://doi.org/10.1073/pnas.77.12.7415.
3. Gessain A, Cassar O. Epidemiological aspects and world distribution of HTLV-1 infection. Front Microbiol. 2012;3:388. https://doi.org/10.3389/fmicb.2012.00388.
4. Araujo AQC, Silva MTT. The HTLV-1 neurological complex. Lancet Neurol. 2006;5(12):1068–76. https://doi.org/10.1016/S1474-4422(06)70628-7.
5. Fuzii HT, da Silva Dias GA, de Barros RJ, Falcão LF, Quaresma JA. Immunopathogenesis of HTLV-1-assoaciated myelopathy/tropical spastic paraparesis (HAM/TSP) - PubMed. https://pubmed.ncbi.nlm.nih.gov/24704970/. Accessed 12 Dec 2023.
6. Alamy AH, Menezes FB, Leite AC, Nascimento OM, Araújo AQ. Dysautonomia in human T-cell lymphotrophic virus type I-associated myelopathy/tropical spastic paraparesis. Ann Neurol. 2001;50(5):681–5. https://doi.org/10.1002/ana.1264.
7. Silva MTT, Mattos P, Alfano A, Araújo AQC. Neuropsychological assessment in HTLV-1 infection: a comparative study among TSP/HAM, asymptomatic carriers, and healthy controls. J Neurol Neurosurg Psychiatry. 2003;74(8):1085–9. https://doi.org/10.1136/jnnp.74.8.1085.
8. Leite ACC, Silva MTT, Alamy AH, et al. Peripheral neuropathy in HTLV-I infected individuals without tropical spastic paraparesis/HTLV-I-associated myelopathy. J Neurol. 2004;251(7):877–81. https://doi.org/10.1007/s00415-004-0455-7.
9. Prince HE, York J, Golding J, Owen SM, Lal RB. Spontaneous lymphocyte proliferation in human T-cell lymphotropic virus type I (HTLV-I) and HTLV-II infection: T-cell subset responses and their relationships to the presence of provirus and viral antigen production. Clin Diagn Lab Immunol. 1994;1(3):273–82. https://doi.org/10.1128/cdli.1.3.273-282.1994.
10. Yasunaga J-i, Sakai T, Nosaka K, et al. Impaired production of naive T lymphocytes in human T-cell leukemia virus type I-infected individuals: its implications in the immunodeficient state. Blood. 2001;97(10):3177–83. https://doi.org/10.1182/blood.v97.10.3177.
11. Matsuoka M, Jeang KT. Human T-cell leukaemia virus type 1 (HTLV-1) infectivity and cellular transformation. Nat Rev Cancer. 2007;7(4):270–80. https://doi.org/10.1038/nrc2111.
12. Nagai M, Yamano Y, Brennan MB, Mora CA, Jacobson S. Increased HTLV-I proviral load and preferential expansion of HTLV-I Tax-specific CD8 + T cells in cerebrospinal fluid from patients with HAM/TSP. Ann Neurol. 2001;50(6):807–12. https://doi.org/10.1002/ana.10065.
13. Macatonia SE, Cruickshank JK, Rudge P, Knight SC. Dendritic cells from patients with tropical spastic paraparesis are infected with HTLV-1 and stimulate autologous lymphocyte proliferation. AIDS Res Hum Retroviruses. 1992;8(9):1699–706. https://doi.org/10.1089/aid.1992.8.1699.
14. Makino M, Wakamatsu S, Shimokubo S, Arima N, Baba M. Production of functionally deficient dendritic cells from HTLV-I-infected monocytes: implications for the dendritic cell defect in adult T cell leukemia. Virology. 2000;274(1):140–8.
15. Hishizawa M, Imada K, Kitawaki T, Ueda M, Kadowaki N, Uchiyama T. Depletion and impaired interferon-alpha-producing capacity of blood plasmacytoid dendritic cells in human T-cell leukaemia virus type I-infected individuals. Br J Haematol. 2004;125(5):568–75. https://doi.org/10.1111/j.1365-2141.2004.04956.x.
16. Nascimento CR, Lima MA, de Andrada Serpa MJ, Espindola O, Leite ACC, Echevarria-Lima J. Monocytes from HTLV-1-infected patients are unable to fully mature into dendritic cells. Blood. 2011;117(2):489–99. https://doi.org/10.1182/blood-2010-03-272690.
17. Echevarria-Lima J, de Abreu Pereira D, de Oliveira TS, et al. Protein profile of blood monocytes is altered in HTLV-1 infected patients: implications for HAM/TSP disease. Sci Rep. 2018;8(1):14354. https://doi.org/10.1038/s41598-018-32324-2.
18. Takeuchi H, Takahashi M, Norose Y, Takeshita T, Fukunaga Y, Takahashi H. Transformation of breast milk macrophages by HTLV-I: implications for HTLV-I transmission via breastfeeding. Biomed Res. 2010;31(1):53–61. https://doi.org/10.2220/biomedres.31.53.
19. Bangham CRM, Araujo A, Yamano Y, Taylor GP. HTLV-1-associated myelopathy/tropical spastic paraparesis. Nat Rev Dis Primers. 2015;1:15012. https://doi.org/10.1038/nrdp.2015.12.
20. Ando H, Sato T, Tomaru U, et al. Positive feedback loop via astrocytes causes chronic inflammation in virus-associated myelopathy. Brain. 2013;136(Pt 9):2876–87. https://doi.org/10.1093/brain/awt183.
21. Enose-Akahata Y, Matsuura E, Tanaka Y, Oh U, Jacobson S. Minocycline modulates antigen-specific CTL activity through inactivation of mononuclear phagocytes in patients with HTLV-I associated neurologic disease. Retrovirology. 2012;9:16. https://doi.org/10.1186/1742-4690-9-16.

22. Gao L, Brenner D, Llorens-Bobadilla E, et al. Infiltration of circulating myeloid cells through CD95L contributes to neurodegeneration in mice. J Exp Med. 2015;212(4):469–80. https://doi.org/10.1084/jem.20132423.
23. Prinz M, Priller J, Sisodia SS, Ransohoff RM. Heterogeneity of CNS myeloid cells and their roles in neurodegeneration. Nat Neurosci. 2011;14(10):1227–35. https://doi.org/10.1038/nn.2923.
24. Jones KS, Petrow-Sadowski C, Huang YK, Bertolette DC, Ruscetti FW. Cell-free HTLV-1 infects dendritic cells leading to transmission and transformation of CD4(+) T cells. Nat Med. 2008;14(4):429–36. https://doi.org/10.1038/nm1745.
25. Azakami K, Sato T, Araya N, et al. Severe loss of invariant NKT cells exhibiting anti-HTLV-1 activity in patients with HTLV-1-associated disorders. Blood. 2009;114(15):3208–15. https://doi.org/10.1182/blood-2009-02-203042.
26. Ziegler-Heitbrock HW. The biology of the monocyte system. Eur J Cell Biol. 1989;49(1):1–12.
27. Ancuta P, Kamat A, Kunstman KJ, et al. Microbial translocation is associated with increased monocyte activation and dementia in AIDS patients. PLoS One. 2008;3(6):e2516. https://doi.org/10.1371/journal.pone.0002516.
28. Veenhuis RT, Williams DW, Shirk EN, et al. Higher circulating intermediate monocytes are associated with cognitive function in women with HIV. JCI Insight. 2021;6(11):e146215. https://doi.org/10.1172/jci.insight.146215.
29. de Castro-Amarante MF, Pise-Masison CA, McKinnon K, et al. Human T cell leukemia virus type 1 infection of the three monocyte subsets contributes to viral burden in humans. J Virol. 2015;90(5):2195–207. https://doi.org/10.1128/JVI.02735-15.
30. Kim FJ, Manel N, Boublik Y, Battini JL, Sitbon M. Human T-cell leukemia virus type 1 envelope-mediated syncytium formation can be activated in resistant mammalian cell lines by a carboxy-terminal truncation of the envelope cytoplasmic domain. J Virol. 2003;77(2):963–9. https://doi.org/10.1128/jvi.77.2.963-969.2003.
31. Williams DW, Calderon TM, Lopez L, et al. Mechanisms of HIV entry into the CNS: increased sensitivity of HIV infected CD14 + CD16 + monocytes to CCL2 and key roles of CCR2, JAM-A, and ALCAM in diapedesis. PLoS One. 2013;8(7):e69270. https://doi.org/10.1371/journal.pone.0069270.
32. Miyoshi I, Kubonishi I, Yoshimoto S, Shiraishi Y. A T-cell line derived from normal human cord leukocytes by co-culturing with human leukemic T-cells. Gan. 1981;72(6):978–81.
33. Daigneault M, Preston JA, Marriott HM, Whyte MKB, Dockrell DH. The identification of markers of macrophage differentiation in PMA-stimulated THP-1 cells and monocyte-derived macrophages. PLoS One. 2010;5(1):e8668. https://doi.org/10.1371/journal.pone.0008668.
34. Yoshikura H, Nishida J, Yoshida M, Kitamura Y, Takaku F, Ikeda S. Isolation of HTLV derived from Japanese adult T-cell leukemia patients in human diploid fibroblast strain IMR90 and the biological characters of the infected cells. Int J Cancer. 1984;33(6):745–9. https://doi.org/10.1002/ijc.2910330606.
35. de Revel T, Mabondzo A, Gras G, Delord B, Roques P, Boussin F, et al. In vitro infection of human macrophages with human T-cell leukemia virus type 1. Blood. 1993;81(6):1598–606. https://doi.org/10.1182/blood.V81.6.1598.1598.
36. Livak KJ, Schmittgen TD. Analysis of relative gene expression data using real-time quantitative PCR and the 2(-delta delta C(T)) method. Methods. 2001;25(4):402–8. https://doi.org/10.1006/meth.2001.1262.
37. Tattermusch S, Skinner JA, Chaussabel D, et al. Systems biology approaches reveal a specific interferon-inducible signature in HTLV-1 associated myelopathy. PLoS Pathog. 2012;8(1):e1002480. https://doi.org/10.1371/journal.ppat.1002480.
38. Gerrick KY, Gerrick ER, Gupta A, Wheelan SJ, Yegnasubramanian S, Jaffee EM. Transcriptional profiling identifies novel regulators of macrophage polarization. PLoS One. 2018;13(12):e0208602. https://doi.org/10.1371/journal.pone.0208602.
39. Davis S, Meltzer PS. GEOquery: a bridge between the Gene expression Omnibus (GEO) and BioConductor. Bioinformatics. 2007;23(14):1846–7. https://doi.org/10.1093/bioinformatics/btm254.
40. Gu Z. Complex heatmap visualization. iMeta. 2022;1(3):e43. https://doi.org/10.1002/imt2.43.
41. Gu Z, Hübschmann D. Pkgndep: a tool for analyzing dependency heaviness of R packages. Bioinformatics. 2022;38(17):4248–51. https://doi.org/10.1093/bioinformatics/btac449.
42. Yunna C, Mengru H, Lei W, Weidong C. Macrophage M1/M2 polarization. Eur J Pharmacol. 2020;877:173090. https://doi.org/10.1016/j.ejphar.2020.173090.
43. Fingleton B. Matrix metalloproteinases as regulators of inflammatory processes. Biochim Biophys Acta Mol Cell Res. 2017;1864(11 Pt A):2036–42. https://doi.org/10.1016/j.bbamcr.2017.05.010.
44. Worley JR, Baugh MD, Hughes DA, et al. Metalloproteinase expression in PMA-stimulated THP-1 cells. Effects of peroxisome proliferator-activated receptor-gamma (PPAR gamma) agonists and 9-cis-retinoic acid. J Biol Chem. 2003;278(51):51340–6. https://doi.org/10.1074/jbc.M310865200.
45. Negishi H, Taniguchi T, Yanai H. The interferon (IFN) class of cytokines and the IFN regulatory factor (IRF) transcription factor family. Cold Spring Harb Perspect Biol. 2018;10(11):a028423. https://doi.org/10.1101/cshperspect.a028423.
46. Lee HC, Lee ES, Uddin MB, et al. Released tryptophanyl-tRNA synthetase stimulates Innate Immune responses against viral infection. J Virol. 2019;93(2):e01291–18. https://doi.org/10.1128/JVI.01291-18.
47. Paley EL, Denisova G, Sokolova O, Posternak N, Wang X, Brownell AL. Tryptamine induces tryptophanyl-tRNA synthetase-mediated neurodegeneration with neurofibrillary tangles in human cell and mouse models. Neuromolecular Med. 2007;9(1):55–82. https://doi.org/10.1385/nmm:9:1:55.
48. Tsai PC, Soong BW, Mademan I, et al. A recurrent WARS mutation is a novel cause of autosomal dominant distal hereditary motor neuropathy. Brain. 2017;140(5):1252–66. https://doi.org/10.1093/brain/awx058.
49. Bogenberger JM, Laybourn PJ. Human T lymphotropic virus type 1 protein tax reduces histone levels. Retrovirology. 2008;5:9. https://doi.org/10.1186/1742-4690-5-9.
50. Nyborg JK, Egan D, Sharma N. The HTLV-1 tax protein: revealing mechanisms of transcriptional activation through histone acetylation and nucleosome disassembly. Biochim Biophys Acta. 2010;1799(3–4):266–74. https://doi.org/10.1016/j.bbagrm.2009.09.002.
51. Amorim CF, Souza AS, Diniz AG, Carvalho NB, Santos SB, Carvalho EM. Functional activity of monocytes and macrophages in HTLV-1 infected subjects. PLoS Negl Trop Dis. 2014;8(12):e3399. https://doi.org/10.1371/journal.pntd.0003399.
52. Rocamonde B, Carcone A, Mahieux R, Dutartre H. HTLV-1 infection of myeloid cells: from transmission to immune alterations. Retrovirology. 2019;16(1):45. https://doi.org/10.1186/s12977-019-0506-x.
53. Yamagishi M, Kubokawa M, Kuze Y, Suzuki A, Yokomizo A, Kobayashi S, Nakashima M, Makiyama J, Iwanaga M, Fukuda T, Watanabe T, Suzuki Y, Uchimaru K. Chronological genome and single-cell transcriptome integration characterizes the evolutionary process of adult T cell leukemia-lymphoma. Nat Commun. 2021;12(1):4821. https://doi.org/10.1038/s41467-021-25101-9.
54. Fuggetta MP, Bordignon V, Cottarelli A, Macchi B, Frezza C, Cordiali-Fei P, Ensoli F, Ciafrè S, Marino-Merlo F, Mastino A, Ravagnan G. Down-regulation of proinflammatory cytokines in HTLV-1-infected T cells by resveratrol. J Exp Clin Cancer Res. 2016;35(1):118. https://doi.org/10.1186/s13046-016-0398-8.
55. Nomura H, Umekita K, Hashikura Y, Umeki K, Yamamoto I, Aratake Y, Saito M, Hasegawa H, Yanagihara K, Okayama A. Diversity of cell phenotypes among MT-2 cell lines affects the growth of U937 cells and cytokine production. Hum Cell. 2019;32(2):185–92. https://doi.org/10.1007/s13577-018-00231-3.
56. Jaworski E, Narayanan A, Van Duyne R, et al. Human T-lymphotropic virus type 1-infected cells secrete exosomes that contain tax protein. J Biol Chem. 2014;289(32):22284–305. https://doi.org/10.1074/jbc.M114.549659.
57. Matsuura E, Enose-Akahata Y, Yao K, et al. Dynamic acquisition of HTLV-1 tax protein by mononuclear phagocytes: role in neurologic disease. J Neuroimmunol. 2017;304:43–50. https://doi.org/10.1016/j.jneuroim.2016.09.014.
58. Suzuki S, Zhou Y, Refaat A, et al. Human T cell lymphotropic virus 1 manipulates interferon regulatory signals by controlling the TAK1-IRF3 and IRF4 pathways. J Biol Chem. 2010;285(7):4441–6. https://doi.org/10.1074/jbc.M109.031476.
59. Yoshita M, Higuchi M, Takahashi M, Oie M, Tanaka Y, Fujii M. Activation of mTOR by human T-cell leukemia virus type 1 tax is important for the transformation of mouse T cells to interleukin-2-independent growth. Cancer Sci. 2012;103(2):369–74. https://doi.org/10.1111/j.1349-7006.2011.02123.x.
60. Gessain A, Mahieux R. Tropical spastic paraparesis and HTLV-1 associated myelopathy: clinical, epidemiological, virological and therapeutic aspects.

Rev Neurol (Paris). 2012;168(3):257–69. https://doi.org/10.1016/j.neurol.2011.12.006.
61. Gajanayaka N, Dong SXM, Ali H, et al. TLR-4 agonist induces IFN-γ production selectively in proinflammatory human M1 macrophages through the PI3K-mTOR- and JNK-MAPK-activated p70S6K pathway. J Immunol. 2021;207(9):2310–24. https://doi.org/10.4049/jimmunol.2001191.
62. Giam CZ, Semmes OJ. HTLV-1 infection and adult T-cell leukemia/lymphoma-a tale of two proteins: tax and HBZ. Viruses. 2016;8(6):161. https://doi.org/10.3390/v8060161.
63. Giam CZ. HTLV-1 replication and adult T cell leukemia development. Recent Results Cancer Res. 2021;217:209–43. https://doi.org/10.1007/978-3-030-57362-1_10.
64. Matsuo M, Ueno T, Monde K, et al. Identification and characterization of a novel enhancer in the HTLV-1 proviral genome. Nat Commun. 2022;13(1):2405. https://doi.org/10.1038/s41467-022-30029-9.
65. Grant C, Jain P, Nonnemacher M, Flaig KE, Irish B, Ahuja J, et al. AP-1-directed human T cell leukemia virus type 1 viral gene expression during monocytic differentiation. J Leukoc Biol. 2006;80(3):640–50. https://doi.org/10.1189/jlb.1205723.
66. Dekkers KF, Neele AE, Jukema JW, Heijmans BT, de Winther MPJ. Human monocyte-to-macrophage differentiation involves highly localized gain and loss of DNA methylation at transcription factor binding sites. Epigenetics Chromatin. 2019;12(1):34. https://doi.org/10.1186/s13072-019-0279-4.
67. Zarei Ghobadi M, Mozhgani SH, Erfani Y. Identification of dysregulated pathways underlying HTLV-1-associated myelopathy/tropical spastic paraparesis through co-expression network analysis. J Neurovirol. 2021;27(6):820–30. https://doi.org/10.1007/s13365-020-00919-z.
68. Ossendorp F, Fu N, Camps M, Granucci F, Gobin SJ, van den Elsen PJ, Schuurhuis D, Adema GJ, Lipford GB, Chiba T, Sijts A, Kloetzel PM, Ricciardi-Castagnoli P, Melief CJ. Differential expression regulation of the alpha and beta subunits of the PA28 proteasome activator in mature dendritic cells. J Immunol. 2005;174(12):7815–22. https://doi.org/10.4049/jimmunol.174.12.7815.
69. Kanada S, Nishiyama C, Nakano N, Suzuki R, Maeda K, Hara M, Kitamura N, Ogawa H, Okumura K. Critical role of transcription factor PU.1 in the expression of CD80 and CD86 on dendritic cells. Blood. 2011;117(7):2211–22. https://doi.org/10.1182/blood-2010-06-291898.
70. Li J, Schuler-Thurner B, Schuler G, Huber C, Seliger B. Bipartite regulation of different components of the MHC class I antigen-processing machinery during dendritic cell maturation. Int Immunol. 2001;13(12):1515–23. https://doi.org/10.1093/intimm/13.12.1515.
71. Jin Y, Fuller L, Ciancio G, et al. Antigen presentation and immune regulatory capacity of immature and mature-enriched antigen presenting (dendritic) cells derived from human bone marrow. Hum Immunol. 2004;65(2):93–103. https://doi.org/10.1016/j.humimm.2003.11.002.
72. Ferrer MF, Thomas P, López Ortiz AO, et al. Junin virus triggers macrophage activation and modulates polarization according to viral strain pathogenicity. Front Immunol. 2019;10:2499. https://doi.org/10.3389/fimmu.2019.02499.
73. Feng J, Cao Z, Wang L, et al. Inducible GBP5 mediates the antiviral response via interferon-related pathways during influenza a virus infection. J Innate Immun. 2017;9(4):419–35. https://doi.org/10.1159/000460294.
74. Shenoy AR, Wellington DA, Kumar P, et al. GBP5 promotes NLRP3 inflammasome assembly and immunity in mammals. Science. 2012;336(6080):481–5. https://doi.org/10.1126/science.1217141.
75. Freitas NL, Gomes YCP, Souza FDS, et al. Lessons from the cerebrospinal fluid analysis of HTLV-1-infected individuals: biomarkers of inflammation for HAM/TSP development. Viruses. 2022;14(10):2146. https://doi.org/10.3390/v14102146.
76. Ma RY, Black A, Qian BZ. Macrophage diversity in cancer revisited in the era of single-cell omics. Trends Immunol. 2022;43(7):546–63. https://doi.org/10.1016/j.it.2022.04.008.

Publisher's Note